The physics impact of proton track identification in future megaton-scale water Cherenkov detectors

The physics impact of proton track identification in future megaton-scale water Cherenkov detectors

M. Fechner[1] and C.W. Walter

Department of Physics, Duke University,
Durham NC 27708, U.S.A.

E-mail: maximilien.fechner@cea.fr, chris.walter@duke.edu

ABSTRACT: In this paper, we investigate the impact in future megaton-scale water Cherenkov detectors of identifying proton Cherenkov rings. We estimate the expected event rates for detected neutral current and charged current quasi-elastic neutrino interactions from atmospheric neutrinos in a megaton-scale Super-Kamiokande-like detector with both 40% and 20% photo-cathode coverage. With this sample we examine the prospects for measuring the neutrino oscillation pattern, and searching for sterile neutrinos. We also determine the size of selected charged current quasi-elastic samples in a 300-kton fiducial volume Super-Kamiokande-like detector from examples of both conventional super-beams and beta-beams proposed in the literature. With these samples, it is shown that full kinematic neutrino reconstruction using the outgoing proton can improve the reconstructed energy resolution, and give good neutrino versus anti-neutrino tagging capabilities, adding important capabilities to water Cherenkov detectors in future projects. We determine the beam parameters necessary to make use of this technique and present distributions of neutrino and anti-neutrino selection efficiencies.

---

[1]Present address: CEA, Irfu, SPP, Centre de Saclay, F-91191, Gif-sur-Yvette, France

Contents

1   Introduction

In [1], it was shown that the particle identification (PID) algorithm of the Super-Kamiokande large water Cherenkov detector [2] could be extended to identify protons. This new tool was used to select single track proton events, mostly produced in neutral current (NC) elastic collisions of atmospheric neutrinos with protons in the water. Proton identification was also used to tag charged-current quasi-elastic (CCQE) atmospheric neutrino events. The importance of being able to identify CCQE events in a water Cherenkov detector is two-fold: it allows full kinematic reconstruction of the neutrino track, and since CCQE

proton production occurs only for neutrinos and not anti-neutrinos, it selects a quasi-pure neutrino sample.

Currently, many new ideas for neutrino experiments are being explored. After the current generation of experiments, new projects to search for CP violation in the neutrino sector and measure the neutrino mass hierarchy may be undertaken [3–5]. These experiments utilize different beams, but all make use of very large detectors. In addition to the neutrinos that come from beams, these large detectors can also study atmospheric and other naturally-produced sources of neutrinos. The capabilities of each detector technology, and the requirements needed to utilize them fully are key issues in designing new facilities. The identification of proton rings is a new capability in water Cherenkov detectors which should be considered when designing these experiments.

Several of the implications of having proton identification in a water Cherenkov detector have been previously explored in [6]. In this work, we use the Super-Kamiokande simulation and reconstruction algorithms to make detailed predictions of the event rate and performance of this technique in future large water Cherenkov detectors exposed to atmospheric and intense artificial beams. We also provide information on efficiencies of detection and photo-cathode coverage requirements which should be of use in future simulation studies.

2 Summary of the proton identification technique

In this work we only briefly summarize the main points of the identification of Cherenkov rings from protons. For a complete description the reader should consult [1].

The main difficulty in identifying protons is separating them from muon tracks, which can have similar ring characteristics, in particular sharp ring edges. Protons tend to interact early in the water, producing shorter tracks than muons. Due to their heavier masses, they also produce Cherenkov rings with smaller opening angles than muons. These observations are used in the separation method. Proton identification is a hypothesis test, used to accept or reject the hypothesis that the observed Cherenkov ring pattern on the photomultiplier tubes (PMTs) of the detector was caused by a proton. A ratio of maximum likelihoods is built from the likelihood of the particle to be a proton, and then a muon. It is then used along with other discriminating variables to make a decision about the particle type.

The first stage of all event processing is a fit of the event vertex, followed by a search for all visible Cherenkov rings. For Super-Kamiokande these steps are described in e.g. [7]. At this stage, the vertex, track direction and Cherenkov cone's opening angle are known, allowing particle identification to be attempted. In the case of a single ring event, the fitted track parameters and the trial particle types are used as inputs to compute the mean expected charges collected by each PMT. This produces the "expected light pattern" of the track configuration under study. This calculation relies on Cherenkov light density tables, which were pre-computed for the relevant particle types using intensive Monte-Carlo simulations. The likelihood of the observed pattern to an expected light pattern can be calculated, and is referred to as a "pattern likelihood". For the proton hypothesis, the pattern likelihood is maximized by adjusting the momentum and track length, yielding the

maximum pattern likelihood $\mathcal{L}_p$. Then, for the muon hypothesis, a fit of the observed light pattern to a muon's expected light pattern is performed, yielding the maximum pattern likelihood $\mathcal{L}_\mu$. The hypothesis test relies on the ratio of the maximum likelihoods $\frac{\mathcal{L}_p}{\mathcal{L}_\mu}$, as well as the best fit estimates of the proton momentum and track length [1].

For CCQE event identification, this method is extended to handle two-prong events, with one lepton and one proton. In principle these should be two-ring events. However studies have shown that CCQE events can confuse the ring finding algorithm: because of the weakness of proton rings when the particle is just above threshold, the reconstruction algorithm often only finds the lepton, although eye-scanning reveals a clear second ring. Therefore CCQE events can be reconstructed either as two-ring or single-ring events. When the ring finding algorithm has identified two rings the hypothesis that the second identified ring is a proton is tested by applying a similar method to the one described above, super-imposing lepton and proton light patterns. For events reconstructed as single ring, the situation is more complicated, since the missing ring must first be identified. A dedicated ring fitter incorporating the proton identification technique was developed and applied to single events, thereby doubling the tagged-CCQE sample size in the atmospheric neutrino sample.

Finally, a set of stringent selection cuts is applied to reduce non-proton backgrounds in the CCQE sample. In order to reduce the non-CCQE background, the full kinematics of the reconstructed final state is used. We use the variable $V^2 = (p_p + p_l - p_N)^2$, where p_p, p_l and p_N are (resp.) the four-momenta of the proton, lepton, and target neutron (assumed to be immobile). Assuming that the reaction is indeed CCQE, a selection cut on V^2 of the outgoing proton-lepton system is made. For a true CCQE event, V^2 is the invariant mass of the incoming neutrino and should then be close to zero. Under the CCQE assumption, non-CCQE events with misidentified or missing particles will have a non-zero invariant mass. Further details on the selection cuts can be found in [1].

This technique was verified by applying it to the Super-Kamiokande atmospheric neutrino data set corresponding to 141 kton years of exposure. Both single protons and CCQE event samples were selected and good agreement was found between data and Monte Carlo. Additionally, a fit to the atmospheric oscillation parameters using this data set found agreement with previously published results [1].

In the remainder of this paper, we will call "tagged-CCQE" events those events with a lepton-like ring and a proton-like ring that pass the selection cuts outlined above.

3 Observability conditions of protons in a water Cherenkov detector

Very close to the Cherenkov threshold, protons can make very weak rings that cannot be detected well. In order to be above Cherenkov threshold, and make enough light to be visible in the detector, the proton momentum must be at least $1.1\,\mathrm{GeV/c}$ [1]. The minimum neutrino energy required to produce such a proton from a CCQE collision in water is approximately $1\,\mathrm{GeV}$. Thus, one requirement for physics studies using CCQE tagging is a high enough event rate above $1\,\mathrm{GeV}$. The efficiency of detection depends on many parameters, including distance from the vertex to the walls of the detector, and is therefore not trivial to estimate. Using a full simulation which accounted for all of these effects, we have produced

the histogram with triangular markers shown in figure 1. The rising response shows the "visibility" of mono-energetic protons in the Super-Kamiokande detector. As expected, it turns-on sharply around $1100\,\mathrm{MeV/c}$ and increases with momentum to reach almost 100%.

However, there is a competing effect: above proton momenta of $\approx 2\,\mathrm{GeV/c}$, which corresponds to neutrino energies above a few GeV, protons often produce secondary particles through hadronic interactions with the water. These secondaries (charged pions or showers from neutral pions) emit Cherenkov light themselves, and impede proper reconstruction due to the presence of extra Cherenkov rings in the event. This probability of producing visible secondaries in the water increases with proton momentum, and makes it almost impossible to identify protons above $\approx 2.5\,\mathrm{GeV/c}$. In figure 1, we also show the fraction of protons that do not produce any visible secondary as a function of momentum (the histogram with square markers) calculated using mono-energetic proton Monte-Carlo events.

Taken together, these two constraints restrict the bounds over which the present technique works well to within the $1.2 - 2.0\,\mathrm{GeV/c}$ momentum range. Therefore, it is not applicable to all beam spectra; it only works for incoming neutrinos with energies of a few GeV.

Also shown in figure 1 is the efficiency of the reconstruction technique for CCQE events (crosses), which we calculated using atmospheric neutrino Monte-Carlo events. As expected from the previous two effects, it peaks around $1.3\,\mathrm{GeV/c}$ and remains appreciable until $\approx 1.9\,\mathrm{GeV/c}$. The efficiency of the CCQE tagging method shown in figure 1 falls to zero more quickly than the combined effect of "visibility" and hadronic interactions because proton patterns become very similar to other track patterns at higher momenta. They therefore fail to pass the selection cuts based on the likelihood fits described above, which further reduces the efficiency even in the absence of secondaries.

4 Neutrino versus anti-neutrino tagging by proton identification

Another great benefit of CCQE tagging by proton identification is that it provides a means of selecting an almost pure neutrino sample. This is due to the fact that in CCQE collisions only neutrinos produce protons in the final state; anti-neutrinos will produce neutrons. The presence of a proton does not guarantee the nature of the incoming neutrino, since other anti-neutrino interaction channels as well as hadronic interactions of neutrons can produce protons. But, even in non-QE events the method preferentially selects neutrino interactions because it picks up protons (and not neutrons) in the final state. Monte-Carlo studies from [1] show that for the Super-Kamiokande atmospheric ν data set, the neutrino fraction of the sample after CCQE selection cuts is $91.7 \pm 3(\mathrm{syst})\%$. Therefore the tagged-CCQE sample is an almost pure neutrino sample when used with atmospheric neutrinos.

Using our Monte-Carlo samples we have calculated the ν and $\bar{\nu}$ selection efficiencies as a function of neutrino energy, i.e. the ratio of all events selected in the tagged-CCQE sample to all events that occur in the detector's fiducial volume (both CCQE and non-CCQE interaction modes are included). These efficiencies are shown in figures 2 and 3, and can be used as input for further simulations. We show the efficiencies for two different values of the photo-cathode coverage of the detector, as this parameter is important for future detector design (see section 5). The peak fraction is $\approx 2\%$ for neutrinos and $\approx 0.5\%$ for anti-
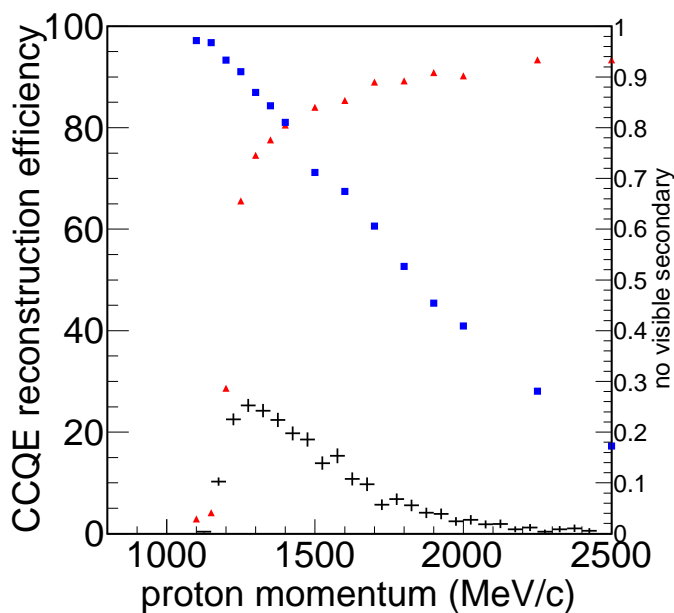
Figure 1. Efficiency of CCQE reconstruction as a function of true proton momentum in MeV/c. The triangles show the fraction of single protons that are visible as a function of proton momentum. This curve has a sharp turn on at the Cherenkov threshold. The square marks show the fraction of protons that do not create visible secondaries in the water, which decreases with momentum, and should be read on the axis on the right hand-side. Those two graphs were calculated using Monte-Carlo simulations of single protons in the detector. The graph with cross markers shows the detection efficiency for CCQE event identification as a function of proton momentum, obtained with the full simulation and reconstruction of simulated atmospheric neutrino events. At higher momenta it is lower than the combined effect of visibility and secondary production because identifying the ring pattern as a proton becomes very difficult as momentum increases.

neutrinos. It is quite low because all detection effects relevant to water Cherenkov detectors are included (data reduction, vertex fitting, ring counting and finally proton selection cuts), along with the high Cherenkov threshold of protons. However, as will be seen, with large exposures, tagged samples of hundreds of events can be expected in future facilities.

This capacity to select neutrinos as opposed to anti-neutrinos will potentially be useful for studies of CP odd matter effects, especially with regard to the neutrino mass hierarchy. Previous studies have investigated the feasibility of such approaches with magnetized iron calorimeters, to separate neutrinos and anti-neutrinos [8]. The new quasi-pure neutrino samples provided by proton tagging open up similar possibilities for large water Cherenkov detectors, although they allow only the selection of neutrino, not pure anti-neutrino samples.

5 Future large water Cherenkov detectors

Several possible future megaton-scale water Cherenkov detectors have been, or are currently being studied in different countries, see for example [5, 9–12]. For a recent review and
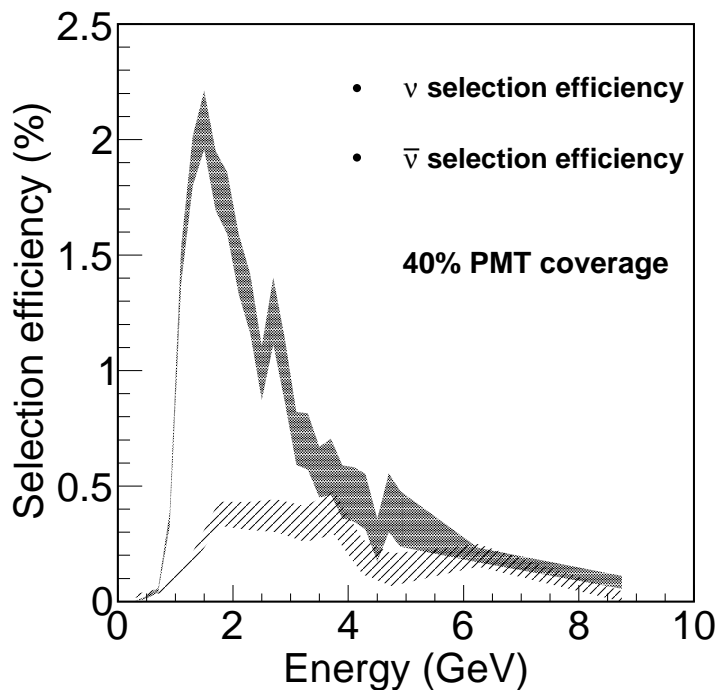
Figure 2. Neutrino and anti-neutrino selection efficiencies as a function of the incoming neutrino energy for 40% photo-cathode coverage (see section 5 for discussion of photo-cathode coverage).
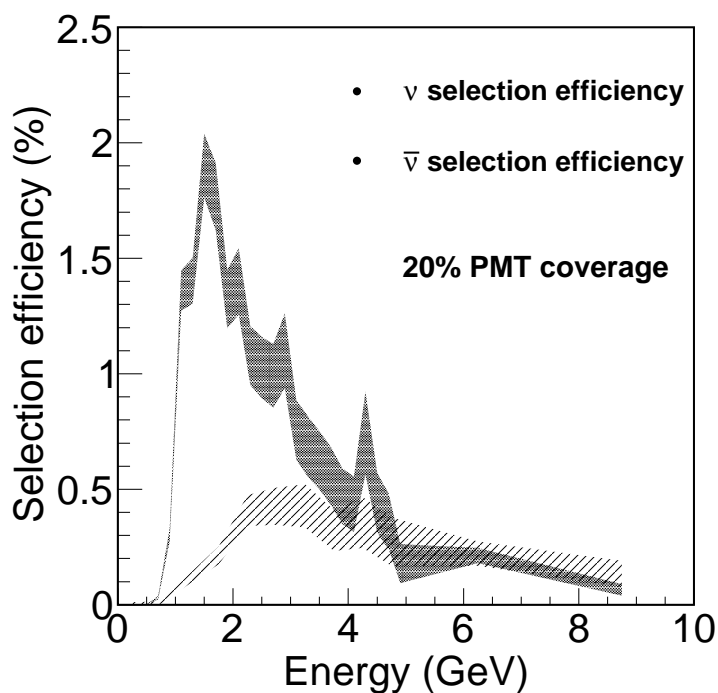
Figure 3. Neutrino and anti-neutrino selection efficiencies as a function of the incoming neutrino energy for 20% photo-cathode coverage (see section 5 for discussion of photo-cathode coverage).

Event class	Expected in 1 Mton yr (40% coverage)	Expected in 1 Mton yr (20% coverage)
Single proton	375	310
Tagged CCQE e-like	337 (53.0%)	295 (51.4%)
Tagged CCQE μ-like	500 (62.4%)	450 (61.3%)

Table 1. Summary of the projected data samples for atmospheric neutrinos: Single proton, tagged-CCQE e-like and tagged-CCQE μ-like, for a Mton-scale detector with efficiencies similar to SK. For tagged-CCQE events the number in parentheses is the fraction of true CCQE events in the selected samples estimated from our Monte-Carlo simulation.

comparison of many of these options the reader is referred to [4]. Using the information gained from our simulations with the Super-Kamiokande detector we have made predictions on the rate of fully reconstructed CCQE events in a water Cherenkov detector for both atmospheric neutrinos and several future intense neutrino beam configurations. We also studied the use of this technique to tag neutrino (as opposed to anti-neutrino) events.

An important question to address when designing a large water Cherenkov detector is the photo-cathode coverage, namely the fraction of the total area of the detector's wall which is instrumented for Cherenkov light collection. Higher coverages induce higher costs. For this purpose, in the studies presented below, we have used the SK simulation to simulate both 40% and 20% photo-cathode coverage. The higher coverage uses the run configuration of 1996-2001, known as SK-I. The lower coverage uses the simulation setup from the run period of 2003 to 2005 (SK-II), following partial reconstruction after an accident in November 2001 that destroyed half the tubes. In what follows we assume that the simulated detectors have the same response as Super-K with these two configurations.

6 Atmospheric neutrinos

6.1 Event rates of proton-tagged atmospheric neutrinos

For determining the expected event rates and detector response from the atmospheric neutrino flux in a future large water Cherenkov detector, the simulations of the Super-Kamiokande detector can simply be scaled by exposure. For an exposure of 1 Mton yr, the gain in statistics would be a factor of ≈ 7 compared to the Super-Kamiokande data set (141 Kton yr). Table 1 summarizes projected estimates of event rates for 1 Mton yr of exposure to atmospheric neutrinos. The predictions for both single-ring proton-like events and tagged-CCQE events are given.

It can be seen in table 1 that a reduction from 40% to 20% photo-cathode coverage would lead to an overall event loss of about 10% for CCQE searches, and about 20% for NC elastic searches.

6.2 Kinematic reconstruction of atmospheric neutrinos

As shown in [1], one of the main appeals of the CCQE tagging technique is accurate kinematic reconstruction of the incoming neutrino track. It is useful for L/E reconstruction,

where L is the neutrino flight path and E its energy. An important feature of L/E reconstruction is its potential for seeing the oscillation shape, and therefore discriminating between oscillation models and other models that could also explain a zenith-dependent flux suppression. In [13], the Super-Kamiokande collaboration performed an L/E analysis using only the lepton momentum (no proton tagging was available). That analysis saw evidence of the oscillatory pattern with high significance. In [1], using the tagged CCQE sample, the Super-Kamiokande collaboration performed another L/E analysis using the reconstructed neutrino information, and found consistent results, albeit with much lower statistics.

A kinematically reconstructed CCQE sample has good resolution in both neutrino energy (approximately 15%) and direction (approximately 12° for ν_μ and 16° for ν_e) according to the studies shown in [1](see table IX). One might naively think that with the improved energy resolution of the proton-tagged CCQE sample with high statistics it would be possible to see the sinusoidal oscillation pattern with even higher resolution than observed in [13]. However, near the horizon, $dL/d\cos\theta_{\rm zenith}$ is very large, and L/E cannot be precisely determined, even with this sample. Figure 4 shows where the first and second oscillation maxima fall in $(\cos\theta_{\rm zenith}, E)$ (dotted and dashed lines), as well as the region where the L/E resolution is worse than 70% (using the same criterion as in [13]) despite kinematic reconstruction (between the quasi-vertical lines). It can be seen that in the energy range spanned by our CCQE atmospheric sample, as constrained by conditions explained in section 3, the first maximum occurs very near the horizon, in a region where L/E precision is low. Even with a Mton-scale Cherenkov detector, the first maximum would remain out of reach. However the second maximum might be visible, but the statistics would remain relatively low (69 expected μ-like events with $-0.6 < \cos\theta_{\rm zenith} < -0.2$ in 1 Mton yr).

6.3 Search for sterile neutrinos using single-proton events

In [1], a sample of single ring proton events was selected, and was shown to be comprised of $\approx 38\%$ of neutral current elastic events $\nu + p \rightarrow \nu + p$. This sample has potential sensitivity to sterile neutrinos, because the proton and the incident neutrino directions are correlated (with a mean scattering angle of $\approx 40°$). Muon neutrinos that are up-going travel a longer path through the Earth and oscillate mainly to ν_τ. Since the neutral current cross-section is flavor-insensitive, the single proton sample is mainly insensitive to $\nu_\mu \rightarrow \nu_\tau$ oscillations. However, if sterile neutrinos exist, and active neutrinos oscillate to sterile neutrinos, a deficit of up-going single-proton events would be observed. To test this hypothesis, the up-down asymmetry $\frac{U-D}{U+D}$ can be calculated. As in [1], up-going events have $-\cos\theta_{\rm zenith} < -0.2$ and down-going events have $-\cos\theta_{\rm zenith} > 0.2$, where $\theta_{\rm zenith}$ is the angle between the proton track and the vertical.

Based on Monte Carlo, the maximum asymmetry is $\approx -15\%$ [1] and would occur if all neutrinos oscillated to sterile neutrinos which has been previously ruled out by [14, 15]. However, models with sterile neutrino admixtures are still the subject of investigation. In such models, some of the ν_μ can oscillate into $\nu_{\rm sterile}$ in addition to the active flavors of neutrinos. With a 1 Mt year exposure, the sample would contain approximately 150 up-going and down-going events (in the absence of sterile neutrinos). The statistical uncertainty on the asymmetry would still be on the order of 6%. Super-Kamiokande has
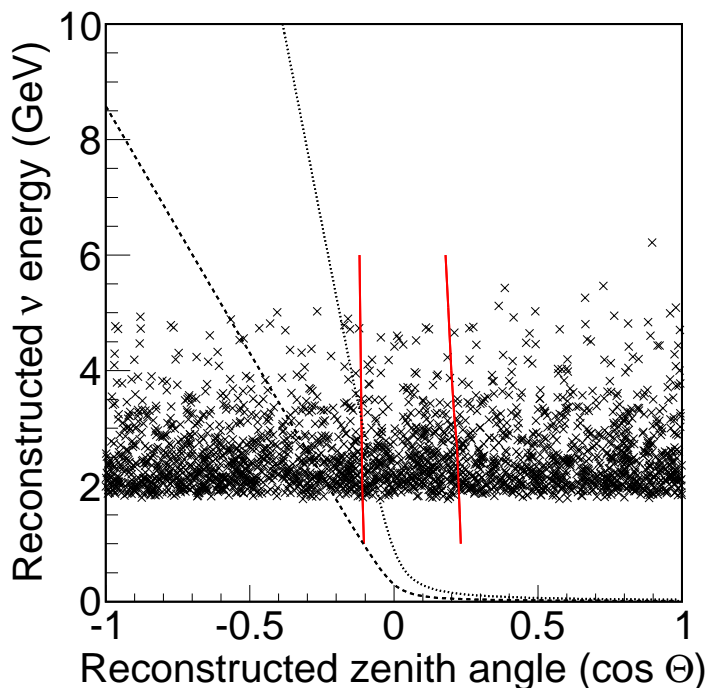
Figure 4. Study of the L/E resolution as a function of reconstructed energy and zenith angle. The region inside the quasi-vertical lines corresponds to an L/E resolution worse than 70%. The dotted and dashed lines indicate the position of the first and second maximum of the oscillation (resp.). The scattered dots show the density of tagged-CCQE Monte-Carlo events at Super-Kamiokande.

previously studied the so-called 2+2 model (see [16]), for which an asymmetry of $\approx -6\%$ is reached for sterile admixtures of $\approx 40\%$. Using other samples, Super-Kamiokande has already ruled out admixtures larger than 26% at 90% CL [17], showing that the single proton event sample does not have enough power on its own to further constrain searches for sterile oscillations, even for a 1Mt year exposure. However, this sample would be a helpful addition to a combined search for sterile neutrinos which used the several different samples sensitive to sterile neutrinos available in water Cherenkov detectors. The numbers quoted above were obtained at 40% photo-cathode coverage. As shown above, at 20% coverage the rates are expected to be roughly 20% lower.

6.4 Summary of expectations with atmospheric neutrinos

In summary, a very large water Cherenkov detector using proton identification would observe several hundreds of NC elastic and CCQE events. The main additions to physics would be the potential visibility of the second oscillation maximum in an L/E analysis, as well as the very high neutrino (as opposed to anti-neutrino) content of the selected CCQE sample, allowing further studies of mass hierarchy effects with atmospheric neutrinos. Sterile neutrino searches based exclusively on this sample would likely not further constrain models beyond the present limits but would be a valuable addition to more comprehensive searches.

lepton flavor	Selected	true-CCQE
e-like	2 ± 0.2	0.5 ± 0.04
μ-like	10.9 ± 0.3	5.9 ± 0.2

Table 2. Expected event selection in the T2K beam for 5×10^{21} protons-on-target, after the selection criteria defined in [1]. The columns labeled true-CCQE show the expected numbers of true CCQE events in the selected sample. We have assumed standard 3-flavor neutrino oscillations, with $\theta_{13} = 0$.

7 Artificially produced neutrino beams

Many new ideas for future neutrino experiments involving large detectors have been studied extensively over the past few years, with a variety of ν production and detection scenarios, including wider band beams with longer baselines (see [3] and references therein). In this section, we study the expected benefits of the CCQE reconstruction method in three examples of upcoming or planned neutrino beams. Our first example will be the T2K experiment's beam which is located in Japan. Then, we study another example of a conventional neutrino beam that could be produced at the future Project-X [18, 19] accelerator complex at Fermilab. Finally, we examine two possible beta-beam configurations. The beam characteristics that we considered and the expected performances are detailed below.

7.1 Tokai to Kamioka (T2K)

This experiment [20] will use a 2.5° off-axis ν_μ beam produced at Tokai (Japan) and detected at Super-Kamiokande (fully rebuilt, with 40% photo-cathode coverage) 295 km away. It will begin in 2009. However the off-axis angle is tuned for a spectrum peak at 0.6 GeV, with the vast majority of neutrinos below 1 GeV, thus making the number of visible protons very small. We estimate that only 24.4 CCQE events would have a visible proton for 5×10^{21} protons on target (40 GeV beam protons). With the same analysis as in [1], only 13.0 events would be selected, half of which would truly be CCQE. Table 2 shows the breakdown as a function of lepton type.

Therefore, we conclude that T2K cannot benefit from CCQE tagging due to the very low statistics. More generally, for a narrow band beam to make use of the CCQE selection technique presented here, protons must be observable, thus the peak energy must be above ≈ 1 GeV, but below a few GeV as explained above.

7.2 The Fermilab to DUSEL Long Baseline Neutrino Experiment (LBNE)

One of the future projects currently under study is a ν_μ beam produced at Fermilab (Illinois, USA), and aimed at the Homestake (South-Dakota, USA) mine 1300 km away, the chosen site for the future Deep Underground Science and Engineering Laboratory (DUSEL). Generically, this experiment is known as the Long Baseline Neutrino Experiment (LBNE). If built, the DUSEL facility could host a Mton-scale water Cherenkov detector. At Fermilab, planning is under way to design a high intensity 2.3 MW neutrino beam based on the Project-X high intensity proton source which could be directed to the DUSEL laboratory. Project-X is built around a 8 GeV superconducting linac which would be paired with

modified versions of the existing accelerator complex at Fermilab to make high intensity neutrino, kaon and muon beams [18, 19].

In the remainder of this section, we have assumed a project-X based neutrino beam with a power of 2.3 MW, using 120 GeV protons. The beam is a wide band beam, and the detector is 1300 km away from the source and 12 km off-axis. We also assumed that 3.6×10^{21} protons were collected, which would correspond to 3 years of running with this beam at full power (about 3×10^7 seconds of live time). The detector used in these calculations is a water Cherenkov detector with a 300-kton fiducial volume, which is assumed to have the same properties (event reconstruction, efficiencies, systematics) as Super-Kamiokande. The beam fluxes are those of [5, 21]. The total integrated neutrino flux over the whole energy range (up to 120 GeV) and 3-year running period is 4.5×10^9 m^{-2} for ν_e and 4.6×10^{11} m^{-2} for ν_μ. For the remainder of this article we will refer to this configuration as the LBNE beam or LBNE project when referring to the beam and detector together.

### 7.2.1 Event rates and purity of CCQE tagged events

Re-weighting the Super-Kamiokande atmospheric Monte-Carlo to the LBNE beam spectrum, we estimate that 750 true-CCQE events with only a single fitted ring will be produced, along with 500 two-ring true-CCQE events (accounting for neutrino oscillations). Using the same selection cuts as for the atmospheric analysis described above, the total tagged-CCQE sample (e-like and μ-like) will contain 750 to 800 events (depending on the PMT coverage), of which about 450 to 470 are truly CCQE. We expect to select roughly 650 μ-like events and 100 e-like events in the tagged-CCQE sample. Although the spectrum extends to over 50 GeV, the neutrino energy is below 5 GeV in the CCQE sample because of the visibility conditions explained in section 3. The average resolution on the measured neutrino energy for this sample is $\approx 15\%$.

In table 1 in section 5, we observed that the selected event rate is reduced by approximately 10% if 20% photo-coverage is used while achieving almost the same CCQE purity as the 40% case. For the LBNE beam, the trend is consistent but precise numbers are difficult to present owing to errors caused by our re-weighting method.

High energy neutrino interactions are a background, especially for ν_e events: the low fraction of CCQE events in the e-like sample is due to the large amount of neutral current π^0 production induced by high energy neutrinos in the wide band beam; gamma showers from π^0 decays fake CCQE ν_e events. Extra techniques for neutral pion background rejection could be applied to select a cleaner ν_e sample, but statistics would be even lower. The value of θ_{13} has a relatively modest influence on the number of selected events: the variation of the e-like sample is on the order of 15% when θ_{13} varies from 0 to 4°, near the expected sensitivity limits of the current generation of experiments.

7.2.2 Energy resolution of CCQE tagged events

One important benefit of CCQE selection is direct neutrino energy reconstruction, with a resolution of about 15% for such a beam. Figure 5 shows the reconstructed spectra for μ-like events in the tank, with and without oscillation. Note that the technique used to kinematically reconstruct the neutrino is different from that which has been used in
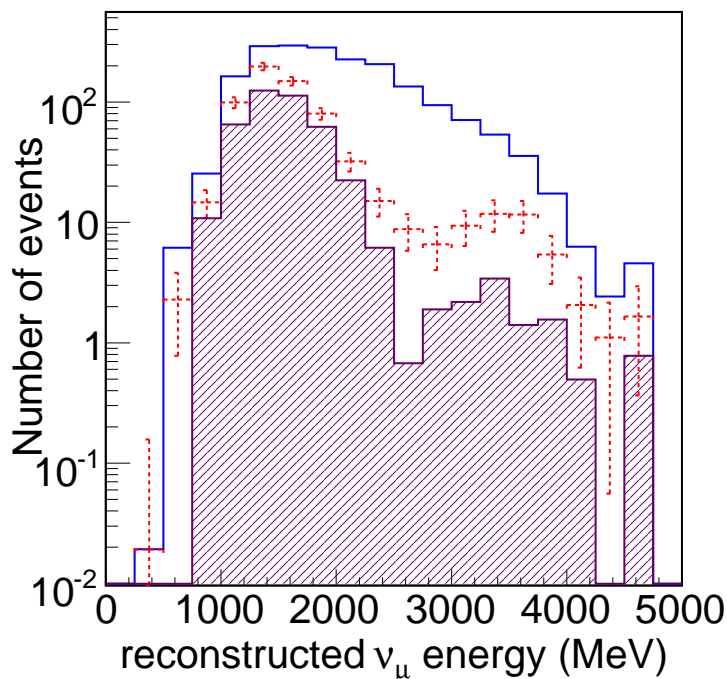
Figure 5. Kinematically reconstructed ν_μ spectrum for the LBNE beam. The full line shows the expectation assuming no oscillation while the dashed points with error bars show the typical expected spectrum with neutrino oscillations, with error bars corresponding to expected statistics. The hatched histogram shows the contribution from true CCQE events.

K2K [22]: here no knowledge of the beam direction is needed since both outgoing particles are known. In section 2 we mentioned that the parameter V^2 (invariant mass of the outgoing lepton system, subtracting the neutron mass) was used to reduce non-CCQE background. With a beam, this cut could also be supplemented by a comparison between the reconstructed neutrino direction and the incoming beam direction to potentially improve non-CCQE rejection. A full study with this requirement would require a dedicated beam flux simulation rather than re-weighted atmospheric Monte-Carlo.

Figure 6 shows the ratio of the oscillated Monte-Carlo to the non-oscillated Monte-Carlo. The error bars reflect the amount of statistics available after 3 years. The oscillatory shape is clearly visible, and shows the good energy resolution reached with this technique. Several sources of systematic errors are expected to affect the oscillatory shape. In [1], a conservative 10% error was used in the relative CCQE selection efficiency. This also includes our imperfect knowledge of the neutrino-nucleus cross-section. This error would distort the oscillatory shape because non-CCQE background will have incorrectly reconstructed energy. Another important source of error comes from inaccuracies and biases in our proton track reconstruction. In [1] they were estimated to be 10%, which is also an overestimate.
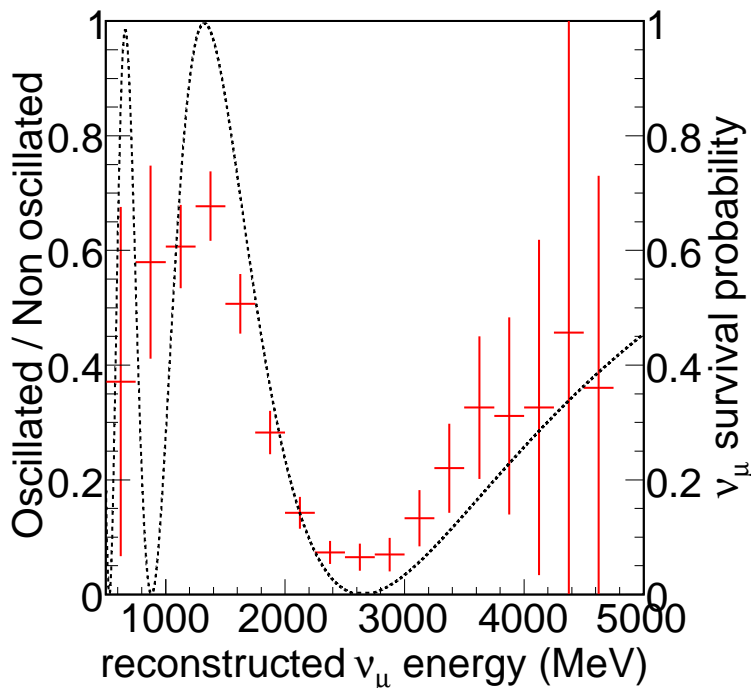
Figure 6. Example of a measurement of the ν_μ oscillation probability as a function of reconstructed neutrino energy: ratio of "measured" spectrum to expected spectrum. The overlaid dashed line is the result of an exact probability calculation, as a function of *true* neutrino energy (explaining the disagreement).

7.2.3 Summary of expectations in the LBNE project

In summary, for this kind of wide-band beam and large detector, the tagged CCQE sample has fairly large statistics of approximately 750-800 events, with a CCQE purity of $\approx 60\%$. The average resolution on the measured neutrino energy for the sample is $\approx 15\%$. The number of tagged-CCQE events selected in the e-like sample will vary between roughly 85 and 100 if θ_{13} varies from 0 to 4 degrees. Although this would not by itself tightly constrain or measure θ_{13}, combining these fully reconstructed events with other samples in a complete analysis would likely be quite helpful.

The ν to $\nu + \bar{\nu}$ ratio in the tagged CCQE sample is estimated to be greater than 98.5%, somewhat improving from the original beam's content (95.5%). Additionally, this technique could be used with the anti-neutrino beam to tag and confirm the neutrino contamination which should be approximately 30% [21].

7.3 Beta-beams

A beta-beam or β-beam [23] is a beam of ν_e or $\overline{\nu}_e$ obtained by accelerating radioactive ions (e.g. ^{18}Ne or ^{6}He) and letting them undergo β decay in a storage ring with long straight sections. The energy of the neutrino follows a boosted β decay spectrum, and the beam is pure ν_e or pure $\overline{\nu}_e$ depending on which element is used.

lepton flavor	Selected	true-CCQE	Selected	true-CCQE
photo-coverage	40%	40%	20%	20%
^{18}Ne ν_e beam				
e-like	2954 ± 117	2009 ± 95	2301 ± 113	1560 ± 82
μ-like	88 ± 20	35 ± 12	115 ± 23	40 ± 13
^{6}He $\overline{\nu}_e$ beam				
e-like	511 ± 92	0	392 ± 82	0
μ-like	93 ± 40	0	44 ± 26	0

Table 3. Expected event selection in a high-energy β-beam at $L = 700$ km and $\gamma = 350$ after the selection criteria defined in [1]. The columns labeled true-CCQE show the expected numbers of true CCQE events in the tagged-CCQE sample. We have assumed standard 3-flavor neutrino oscillations, with $\theta_{13} = 0$.

The performances depend on the end-point E_0 of the β-decay spectrum, i.e. on the ion; they also depend on the baseline L between the accelerator and the detector, and the relativistic γ factor of the ions. Many combinations of these three parameters have been considered for future facilities, and the reader should consult e.g. [3] for a summary of all the available options.

In order to reach neutrino energies of a few GeV, so as to make visible protons, the relevant options would be $L = 700$ km and $\gamma = 350$, with ^{18}Ne (for ν_e production, with $E_0 = 3423.7$ keV) and ^{6}He (for $\overline{\nu}_e$ production, with $E_0 = 3506.7$ keV). Such options (so called high-energy β-beams) could correspond to a refurbished SPS (at CERN) or Tevatron (at FNAL). We have assumed that the ion fluxes were 2.9×10^{18} decays per year for He ions and 1.1×10^{18} decays per year for Ne ions, following the EURISOL β-beam group quoted in [3]. This configuration yields a flux peak at ≈ 1.6 GeV and a spectrum endpoint at ≈ 2.4 GeV. The total integrated flux per year is 6.5×10^{11} m^{-2} for $\overline{\nu}_e$ and 2.4×10^{11} m^{-2} for ν_e.

7.3.1 Event rates and purity of CCQE tagged events

Re-weighting the SK atmospheric Monte-Carlo to the β-beam spectra, and applying the same analysis as for the LBNE project we have obtained the numbers in table 3 which correspond to an exposure of 900 kton-year. The event rates are about four times higher than for the LBNE beam studied in the previous section due to the higher flux. Running in pure $\overline{\nu}_e$ mode would ensure that there would be no neutrino CCQE events, which could provide a separate measurement of the various background events that contaminate the neutrino CCQE sample when running with ν_e. Our Monte-Carlo simulations show that $\approx 33\%$ of the tagged-CCQE $\bar{\nu}$ events are $\bar{\nu}$-CCQE events, i.e. $\bar{\nu} + p \rightarrow \text{lepton} + n$. These events are tagged because the outgoing neutron interacted hadronically with the detector's water and produced a proton. Approximately 43% of the $\bar{\nu}$ tagged-CCQE sample comes from charged-current single-pion production (especially $\bar{\nu} + p \rightarrow \text{lepton} + p + \pi^-$, detecting the outgoing proton), $\approx 13\%$ comes from neutral-current single-pion production, and $\approx 9\%$ from charged-current multi-pion production.
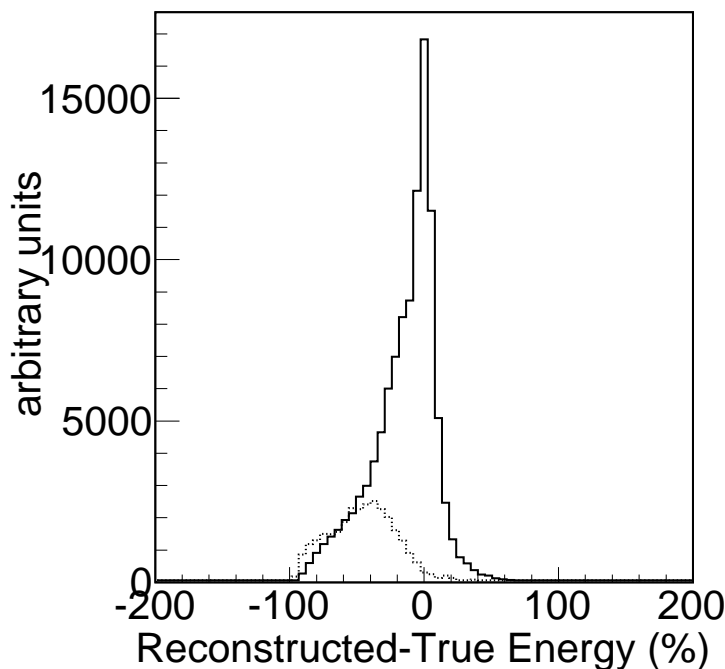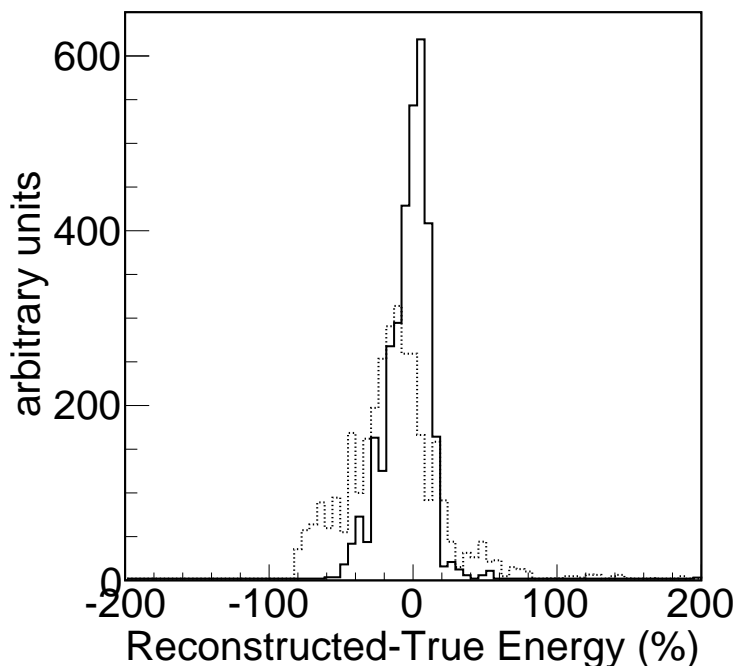
Figure 7. Neutrino energy resolution for ν_e β-beam single-ring (full line) and two-ring (dashed line) e-like events. There is no proton tagging, and only the lepton information is used to estimate the neutrino energy.

7.3.2 Energy resolution of CCQE tagged events

As with the wide-band superbeam described in the previous sub-section, kinematic reconstruction of the incoming neutrino also improves the energy resolution. Figure 7 shows the energy resolutions that can be expected with the ν_e β-beam, selecting all single-ring e-like events, without any proton tagging, which is the usual method for neutrino energy estimation in water Cherenkov detectors. The neutrino energy is obtained from the beam direction and the lepton information alone as in e.g. the K2K experiment [22]. This energy reconstruction method assumes that all events are CCQE, and therefore any contamination with non CCQE events leads to an error on the measured energy, usually an underestimate. In figure 7, a narrow peak corresponding to correctly identified CCQE events with good resolution is visible, along with a large tail of non-CCQE events. It can be seen that two-ring events (dashed line) are almost always mis-reconstructed with this method because they are largely non-CCQE. They cannot be used when reconstructing the neutrino energy with lepton information alone.

By contrast, figure 8 shows the effect of using proton tagging and full kinematic neutrino energy reconstruction with the two tracks. The two methods for reconstructing the neutrino energy, either full kinematic reconstruction with the proton and lepton track, or reconstruction with the lepton track alone as shown in figure 7, are compared. In this figure only tagged-CCQE events were used, in order to show the improvement brought by proton tagging. The energy resolution on the incoming neutrino obtained using this technique as demonstrated in figure 8 is $\approx 11\%$.

Figure 8. Neutrino energy resolution for the tagged-CCQE sample from the ν_e β-beam. The dotted line corresponds to reconstruction using the lepton information only, and the full line to full kinematic reconstruction using the proton and the lepton.

7.3.3 Summary of expectations in the beta-beam

In summary, reconstructing the proton track eliminates non-CCQE events very efficiently, makes use of the two-ring sample, and has good energy resolution, but the requirements on proton visibility strongly reduce the statistics. The main interest of this technique for a β-beam is to select a high resolution, $\approx 66\%$ pure CCQE sample.

8 Conclusion

In this paper, we studied the physics potential of a novel proton identification technique in future large water Cherenkov detectors, with atmospheric neutrinos and several possible neutrino beam scenarios. We used the SK-I (40% photo-cathode coverage) and SK-II (20% photo-cathode coverage) simulations, which have been carefully tuned on atmospheric neutrino data, and re-weighted them to match various neutrino flux spectra.

For atmospheric neutrinos, a megaton scale Cherenkov detector utilizing this technique would observe several hundred NC elastic and CCQE events. The energy resolution of the sample is excellent, but the selected energy of the sample has the first oscillation maximum near the horizon where the resolution is still poor. However, the second oscillation maximum pattern might still be visible albeit with relatively low statistics. There will be a quasi-pure neutrino sample, allowing further studies of mass hierarchy effects with atmospheric neutrinos. We find that, for this analysis, decreasing the photo-cathode coverage from 40% to 20% decreases the event rate by approximately 10% for CCQE searches

and 20% for NC searches in atmospheric neutrinos. The purity of the CCQE sample is little changed however. Finally, sterile neutrino searches based on this sample would be a valuable addition to more comprehensive searches.

We also studied how the proton identification and CCQE selection techniques could be applied to neutrino beams. In order to have significant statistics, the beam must have a high event rate in the few GeV region, between 1 and 5 GeV. A wide band superbeam of the kind envisioned in the LBNE project would produce a sample of a few hundred events, while a beta-beam would produce a few thousand. In both cases, the newly selected sample provides a direct measurement of the neutrino energy using event kinematics, with good resolution (10-15%). In both cases the proton tag can be used to either purify the neutrino beam or measure the neutrino contamination in the anti-neutrino beam.

Water Cherenkov detectors are in general chosen because of their cost-effectiveness, and because they are a mature technology. However they are known to have several limitations (see e.g. [3]). Single ring event detection is emphasized since, by using the lepton direction and incoming neutrino direction alone, the energy of the neutrino can be reconstructed. It is assumed that CCQE and non-CCQE events in this sample cannot be separated. Consequently, the neutrino beams usually studied with water Cherenkov detectors are often limited to energies of 1 GeV or less to avoid contaminating the sample with too many non-CCQE events which spoil neutrino energy reconstruction.

Moreover, water Cherenkov detectors are thought to be unable to detect whether the incoming neutrino is a neutrino or an anti-neutrino, mainly because this capability relies on measuring the sign of the outgoing charged lepton and requires a magnetized detector. These limitations render them less attractive than other detection technologies (e.g. liquid argon) for CP violation studies, where these distinctions can be crucial.

We have shown here that these limitations can be partially lifted by careful analysis of the Cherenkov light patterns: the non-CCQE contamination can be reduced, CCQE events can be tagged, and the neutrino can be kinematically reconstructed, ensuring at the same time that it is a neutrino and not an anti-neutrino. We have also shown that beam spectra with peak energies in the few GeV region are needed for these studies. The exact quantitative effect on the sensitivity to the mass hierarchy or $\delta_{\rm CP}$ is beyond the scope of this work and depends on the exact beam and detector configuration along with their locations. However, we have shown it is possible to obtain a few hundred atmospheric neutrino events, and depending on the beams, from a few hundred to a few thousand events in a megaton scale water Cherenkov detector.

As an example of another possible impact of this technique we note that in [24], the authors show in a low-energy neutrino factory, ν to $\nu+\bar{\nu}$ ratios of $50-90\%$ are enough to reach good sensitivity to CP-violation and the mass hierarchy, provided that $\sin^2 2\theta_{13} > 10^{-3}$. Also, in [25], the author explains that even a modest statistical separation between neutrinos and anti-neutrinos in a large detector with particle identification can have dramatic impact on the sensitivity to the mass hierarchy either using atmospheric neutrinos alone, or combined with long-baseline results. We hope that these new capabilities of water Cherenkov detectors will be useful when designing these future facilities.

Acknowledgments

References

[1] SUPER-KAMIOKANDE collaboration, M. Fechner et al., *Kinematic reconstruction of atmospheric neutrino events in a large water Cherenkov detector with proton identification*, *Phys. Rev.* **D 79** (2009) 112010 [arXiv:0901.1645] [SPIRES].

[2] Y. Fukuda et al., *The Super-Kamiokande detector*, *Nucl. Instrum. Meth.* **A 501** (2003) 418 [SPIRES].

[3] ISS PHYSICS WORKING GROUP collaboration, A. Bandyopadhyay et al., *Physics at a future Neutrino Factory and super-beam facility*, *Rept. Prog. Phys.* **72** (2009) 106201 [arXiv:0710.4947] [SPIRES].

[4] ISS DETECTOR WORKING GROUP collaboration, T. Abe et al., *Detectors and flux instrumentation for future neutrino facilities*, 2009 *JINST* **4** T05001 [arXiv:0712.4129] [SPIRES].

[5] V. Barger et al., *Report of the US long baseline neutrino experiment study*, arXiv:0705.4396 [SPIRES].

[6] J.F. Beacom and S. Palomares-Ruiz, *Neutral-current atmospheric neutrino flux measurement using neutrino proton elastic scattering in Super-Kamiokande*, *Phys. Rev.* **D 67** (2003) 093001 [hep-ph/0301060] [SPIRES].

[7] SUPER-KAMIOKANDE collaboration, Y. Ashie et al., *A Measurement of Atmospheric Neutrino Oscillation Parameters by Super-Kamiokande I*, *Phys. Rev.* **D 71** (2005) 112005 [hep-ex/0501064] [SPIRES].

[8] D. Indumathi and M.V.N. Murthy, *A question of hierarchy: Matter effects with atmospheric neutrinos and anti-neutrinos*, *Phys. Rev.* **D 71** (2005) 013001 [hep-ph/0407336] [SPIRES].

[9] A. de Bellefon et al., *MEMPHYS: A large scale water Cerenkov detector at Frejus*, hep-ex/0607026 [SPIRES].

[10] M. Goodman et. al., *Physics Potential and Feasibility of UNO*, PREPRINT-SBHEP01-3.

[11] K. Nakamura, *Hyper-Kamiokande: A next generation water Cherenkov detector*, *Int. J. Mod. Phys.* **A 18** (2003) 4053 [SPIRES].

[12] M. Diwan et al., *Proposal for an experimental program in neutrino physics and proton decay in the homestake laboratory*, hep-ex/0608023 [SPIRES].

[13] SUPER-KAMIOKANDE collaboration, Y. Ashie et al., *Evidence for an oscillatory signature in atmospheric neutrino oscillation, Phys. Rev. Lett.* **93** (2004) 101801 [`hep-ex/0404034`] [SPIRES].

[14] SUPER-KAMIOKANDE collaboration, S. Fukuda et al., *Tau neutrinos favored over sterile neutrinos in atmospheric muon neutrino oscillations, Phys. Rev. Lett.* **85** (2000) 3999 [`hep-ex/0009001`] [SPIRES].

[15] MINOS collaboration, P. Adamson et al., *Search for active neutrino disappearance using neutral- current interactions in the MINOS long-baseline experiment, Phys. Rev. Lett.* **101** (2008) 221804 [`arXiv:0807.2424`] [SPIRES].

[16] G.L. Fogli, E. Lisi and A. Marrone, *Four-neutrino oscillation solutions of the atmospheric neutrino anomaly, Phys. Rev.* **D 63** (2001) 053008 [`hep-ph/0009299`] [SPIRES].

[17] SUPER-K collaboration, C.W. Walter, *Distinguishing $\nu_\mu \rightarrow nu/tau$ oscillations and exotic oscillation/decay hypotheses using Super-K atmospheric neutrino data, Nucl. Instrum. Meth.* **A 503** (2003) 110 [SPIRES].

[18] J. Appel et al., *Physics with a high intensity proton source at Fermilab*, (2008) http://www.fnal.gov/directorate/Longrange/Steering_Public/P5/GoldenBook-2008-02-03.pdf.

[19] S. Holmes, *Project X Initial Configuration Document*, (2008) http://projectx-docdb.fnal.gov/cgi-bin/RetrieveFile?docid=83&extension=pdf.

[20] THE T2K collaboration, Y. Itow et al., *The JHF-Kamioka neutrino project*, [`hep-ex/0106019`] [SPIRES].

[21] M. Bishai et al., private communication.

[22] K2K collaboration, M.H. Ahn et al., *Measurement of Neutrino Oscillation by the K2K Experiment, Phys. Rev.* **D 74** (2006) 072003 [`hep-ex/0606032`] [SPIRES].

[23] P. Zucchelli, *A novel concept for a anti-nu/e/nu/e neutrino factory: The beta beam, Phys. Lett.* **B 532** (2002) 166 [SPIRES].

[24] P. Huber and T. Schwetz, *A low energy neutrino factory with non-magnetic detectors, Phys. Lett.* **B 669** (2008) 294 [`arXiv:0805.2019`] [SPIRES].

[25] T. Schwetz, *Physics Potential of Future Atmospheric Neutrino Searches, Nucl. Phys. Proc. Suppl.* **188** (2009) 158 [`arXiv:0812.2392`] [SPIRES].